Lab on a Chip

Miniaturisation for chemistry, biology & bioengineering

www.rsc.org/loc

Volume 9 | Number 6 | 21 March 2009 | Pages 741–848

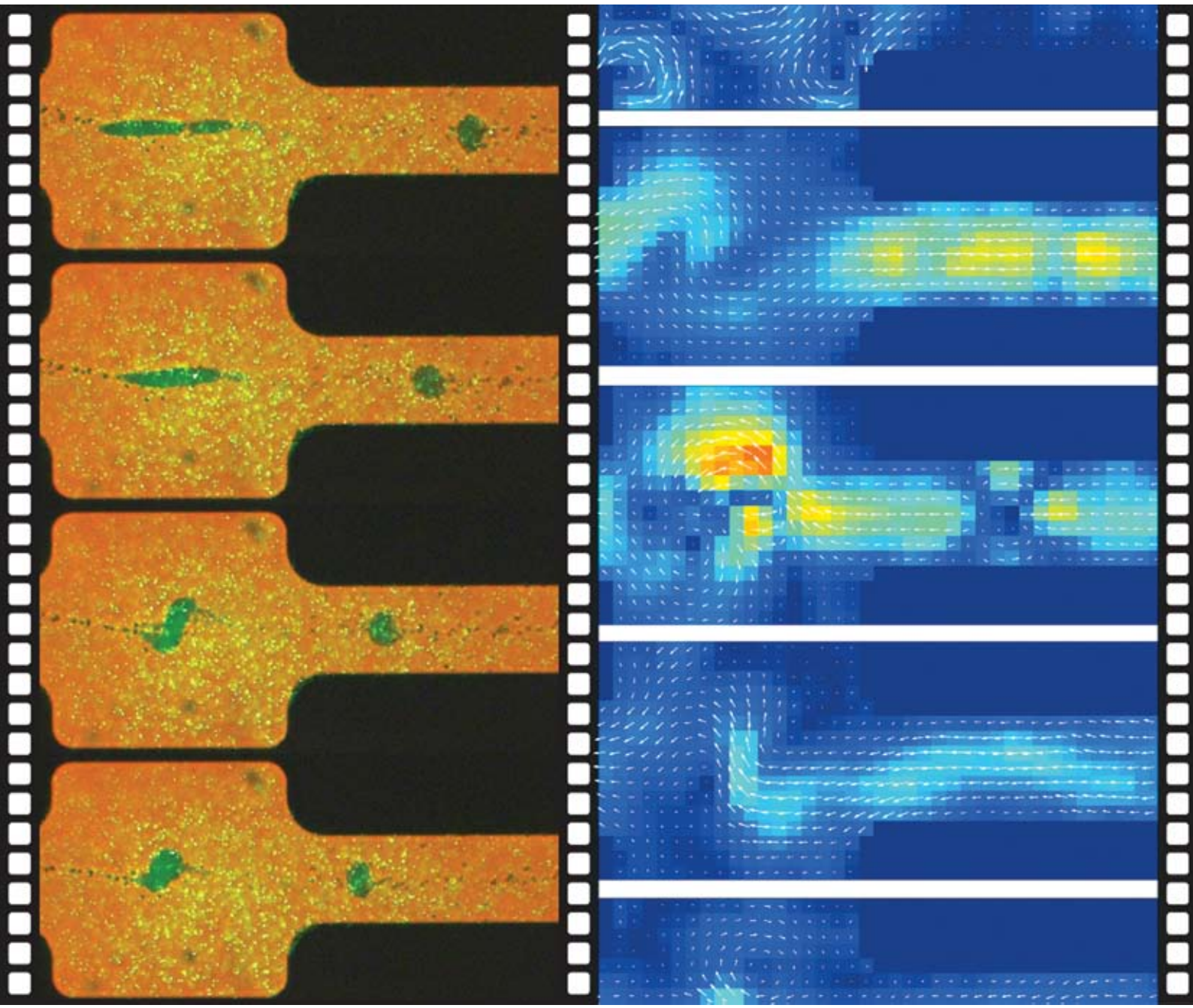

ISSN 1473-0197

RSC Publishing

1473-0197(2009)9:6;1-W

Flow-free transport of cells in microchannels by frequency-modulated ultrasound†

O. Manneberg,[a] B. Vanherberghen,[a] B. Önfelt[ab] and M. Wiklund*[a]

Received 13th October 2008, Accepted 9th January 2009
First published as an Advance Article on the web 2nd February 2009
DOI: 10.1039/b816675g

We demonstrate flow-free transport of cells and particles by the use of frequency-modulated ultrasonic actuation of a microfluidic chip. Two different modulation schemes are combined: A rapid (1 kHz) linear frequency sweep around ~6.9 MHz is used for two-dimensional spatial stabilization of the force field over a 5 mm long inlet channel of constant cross section, and a slow (0.2–0.7 Hz) linear frequency sweep around ~2.6 MHz is used for flow-free ultrasonic transport and positioning of cells or particles. The method is used for controlling the motion and position of cells monitored with high-resolution optical microscopy, but can also be used more generally for improving the robustness and performance of ultrasonic manipulation micro-devices.

Introduction

Flow-free transport and positioning of cells in microfluidic systems is important for studies of processes such as cellular release of signaling molecules, intercellular communication and cell proliferation.[1] Available methods for controlled translation of cells relative to the fluid medium in a microchannel are, *e.g.*, dielectrophoresis[2] and optoelectronic tweezers.[3] However, these methods are either bulky, expensive or complex, and they suffer from limited biocompatibility. In the present paper we present a simple method for flow-free cell transport in a microchannel based on frequency-modulated ultrasonic actuation.

Forces generated by resonant acoustic fields can be used for manipulation of cells or other micrometer-sized particles in microfluidic chips. In particular, the method has shown to be attractive and efficient in flow-through-operation applications such as continuous alignment, separation and enrichment of cells[4] and bio-functionalized beads.[5] On the other hand, frequency-modulated ultrasonic actuation has previously been employed in flow-free macro-scale (>1 mm) chambers for transportation and positioning of suspended particles. Examples include simultaneous actuation at two slightly different frequencies for either translation[6,7] or confinement[8] of trapped particles. Furthermore, different schemes for sweeping or changing a single actuation frequency have been used for translation or merging of particle aggregates.[9,10] However, it is not straightforward to implement frequency-modulation methods in microfluidic chips. In order to realize flow-free particle transport by ultrasound in a chip, the spatial distribution of the generated force field must be pre-controlled along the whole microchannel. In contrast, recent evaluations have shown that the commonly employed design for ultrasonic manipulation in a chip (the half-wavelength-wide channel) does not focus particles uniformly along the length of the channel.[11,12] Instead, the focusing forces along the channel typically vary between being positive (alignment), zero (no effect) and negative (de-alignment). Since an acoustic particle separator[4] operated with a significant fluid flow is only dependent on the net effect along the full channel, this problem has previously not been considered or known. For flow-free transport purposes, however, spatial stabilization of the pre-alignment forces is crucial.

In the present paper we demonstrate flow-free transport of cells and other particles in a microfluidic chip by the use of frequency-modulated ultrasonic actuation. We combine two modulation strategies: Rapid frequency sweeping for stabilized particle alignment in two dimensions; and slow frequency sweeping for flow-free particle transport along a microchannel. The method is used for controlled transport, merging and optical characterization of ultrasonically caged[13] human immune and kidney cells. We conclude that rapid frequency sweeping is a simple approach for improving the robustness of an ultrasound-actuated microfluidic chip, with benefits such as reduced temperature dependence and less need for trimming/controlling the actuation frequency. Furthermore, rapid frequency sweeping is also a prerequisite for accurate particle transport over several millimeters, which here is realized by a combined rapid and slow frequency sweeping approach.

Methods

Fig. 1 shows the experimental arrangement. It is similar to the one in Ref. 13, but with the modification that the two excitation signals (around 2.6 and 6.9 MHz) were modulated by a sawtooth-shaped frequency sweep. In brief, the chip includes a $5 \times 0.11 \times 0.11$ mm^3 inlet channel for two-dimensional (2D) alignment, arraying[11] and transport of particles or cells, and a $0.30 \times 0.30 \times 0.11$ mm^3 filleted square box for three-dimensional (3D) caging[13] of particles or cells. The wedge transducers employed were designed and fabricated according to the

[a]*Department of Applied Physics, Royal Institute of Technology, AlbaNova University Center, SE-106 91 Stockholm, Sweden. E-mail: martin@biox.kth.se*
[b]*Department of Microbiology, Tumor and Cell Biology, Karolinska Institutet, SE-171 77 Stockholm, Sweden*

† Electronic supplementary information (ESI) available: Real-time videos of ultrasound-mediated transport of cells and particles, and time-resolved particle image velocimetry (PIV) of the fluid motion during particle transport. See DOI: 10.1039/b816675g

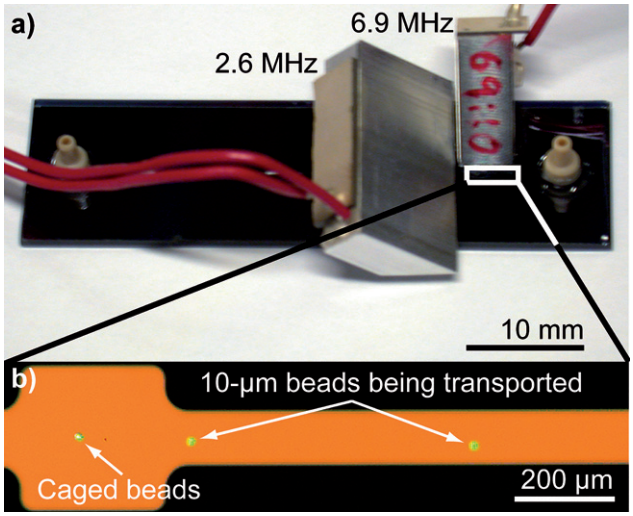

Fig. 1 (a): A photo of the chip (further described in Ref. 13) with mounted wedge transducers (further described in Ref. 11); a 6.9 MHz transducer for particle alignment, and a 2.6 MHz transducer for particle transport and caging. (b): A micrograph showing part of the 5 mm long inlet channel for alignment and transport of particles (to the right), and the cage for trapping and positioning of particles (to the left).

procedure described in Ref. 11, and operated at 10 V_{pp}. For stabilization of the 2D alignment in the inlet channel, the 6.9 MHz transducer was driven in linear sweeps from 6.85 to 6.95 MHz at a rate of 1 kHz (rapid modulation). For particle transport, the 2.6 MHz transducer was driven in linear sweeps from 2.60 to 2.64 MHz at a rate of 0.2, 0.5 or 0.7 Hz (slow modulation), while the 6.9 MHz transducer was driven in linear sweeps from 6.90 to 7.00 MHz at a rate of 1 kHz (rapid modulation). In the experiments, 1 and 5 μm polymer beads were used for visualizing the fluid flow and the acoustic force fields, respectively, and 10 μm polymer beads, human embryonic kidney (HEK 293T) cells and natural killer (NK) cells isolated from peripheral blood were used for proof-of-concept demonstration of the target application of our device. The fluid motion during transport was characterized by the particle image velocimetry (PIV) package "MPIV"[14] executed on consecutive frame pairs from a video captured during several periods of the frequency modulation.

Results

Fig. 2 demonstrates the effect of stabilizing the 2D alignment function by use of rapid modulation of the 6.9 MHz transducer. Initially, the ~5 mm long inlet channel is seeded with a uniform distribution of 5 μm beads, and each image is acquired after 5 s of ultrasonic actuation without any fluid flow. In Fig. 2a–f, the result is shown for six single (non-modulated) frequencies within the investigated interval 6.85–6.95 MHz. We note that all single-frequency patterns contain several "blind spots" of different sizes, which are characterized by weak forces unable to align the beads within the 5 s (*cf. e.g.* at the white arrow in Fig. 2c). Interestingly, while all investigated frequencies can align the beads very efficiently at some locations, the relative total length of the blind spots over the full inlet channel still varies between approximately 20% (Fig. 2c) and 60% (Fig. 2e). Furthermore, certain frequencies also have areas where the beads are driven towards, and not away from the channel walls ("de-alignment", *cf. e.g.* at the yellow arrow in Fig. 2c).

In Fig. 2g, the actuation frequency is swept linearly from 6.85 to 6.95 MHz at a rate of 1 kHz. We see that the result of this rapid modulation is uniform alignment of the beads into the vicinity of the midpoint of the channel cross section over the entire inlet channel. It is noted that up to ~5% of the inlet channel still has slightly weaker forces causing incomplete alignment. However, if the actuation time is increased to 10 s, all beads can be aligned during no-flow conditions (data not shown).

In Fig. 3a, we demonstrate flow-free transport of aggregates of 5 μm beads simultaneously with stabilized 2D alignment. (The micrographs in Fig. 3a are selected frames from the first ESI video clip.)† Here, the 2D alignment is performed by rapid modulation (6.90–7.00 MHz; rate 1 kHz), and the particle transport is realized by slow modulation (2.60–2.64 MHz; rate 0.5 Hz). Fig. 3b quantifies the distance d traveled along the channel as a function of time t for one aggregate at three different sweep rates (0.2, 0.5 and 0.7 Hz). As can be seen in the inset in Fig. 3b, the transport speed scales linearly with the modulation frequency. The maximum modulation frequency for achieving effective transport of the aggregates shown in Fig. 3a turned out to be 0.7 Hz, which corresponds to a transport speed of 0.2 mm s^{-1}. Finally, in Fig. 3c we demonstrate controlled transport and caging of individual HEK cells (first three panels), and a fluorescence image of a single

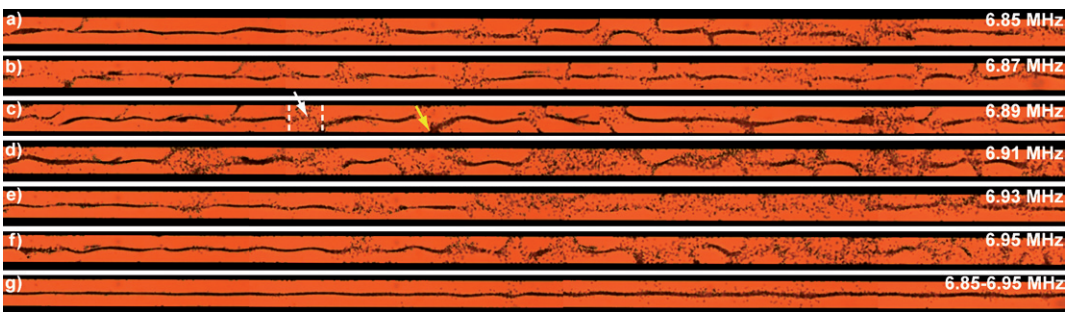

Fig. 2 Fixed-frequency operation (a–f) compared with modulated-frequency operation (g) of the 6.9 MHz transducer when the inlet channel is filled with 5 μm beads (10 V_{pp} actuation during 5 s without fluid flow). The white arrow marks a "blind spot" having insignificant forces, and the yellow arrow marks an area of "de-alignment" where the particles are driven to the channel walls.

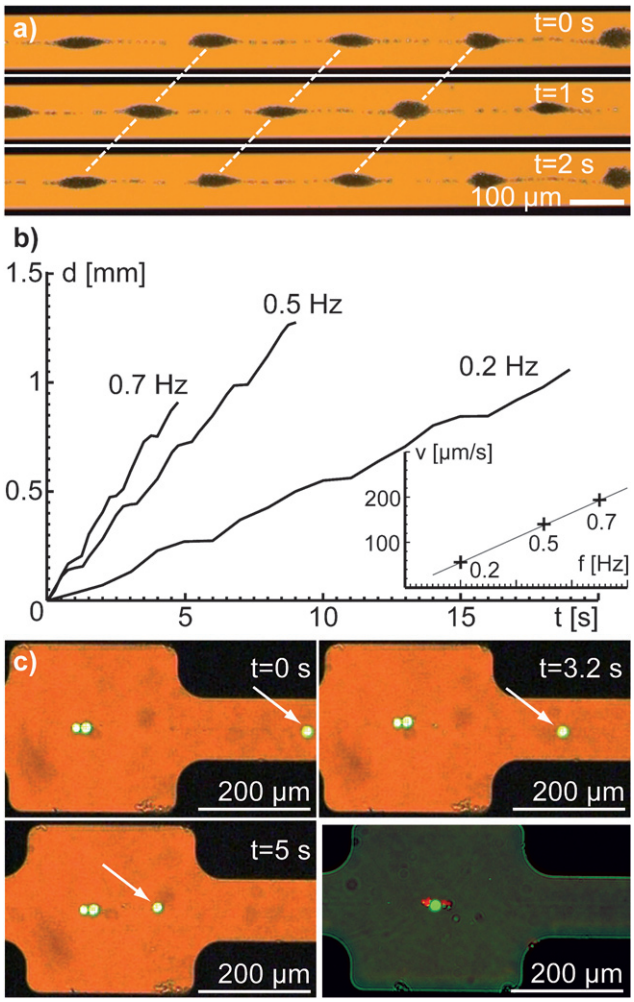

Fig. 3 (a): Three frames from a video clip (provided as ESI)† demonstrating ultrasound-mediated arraying and transport of aggregates of 5 µm beads without fluid flow (sweep rate 0.5 Hz). The dotted line indicates corresponding aggregates between the frames. (b): Quantification of the distance *d* traveled along the channel for the aggregates in (a) as a function of time *t* for different sweep rates. The inset plots the slope of a linear fit to each distance-*versus*-time curve (*i.e.*, the velocity *v*) as a function of the sweep rate *f*. (c): Demonstration of ultrasound-mediated transport for individual cell injection into the ultrasonic cage. The first three panels show sequential merging and positioning of three HEK cells without fluid flow (also provided as ESI),† and the last panel shows a caged HEK/NK-cell conjugate monitored by fluorescence microscopy. The HEK cells and NK cells are labeled with green- and red-fluorescent viability indicators calcein-AM, respectively.

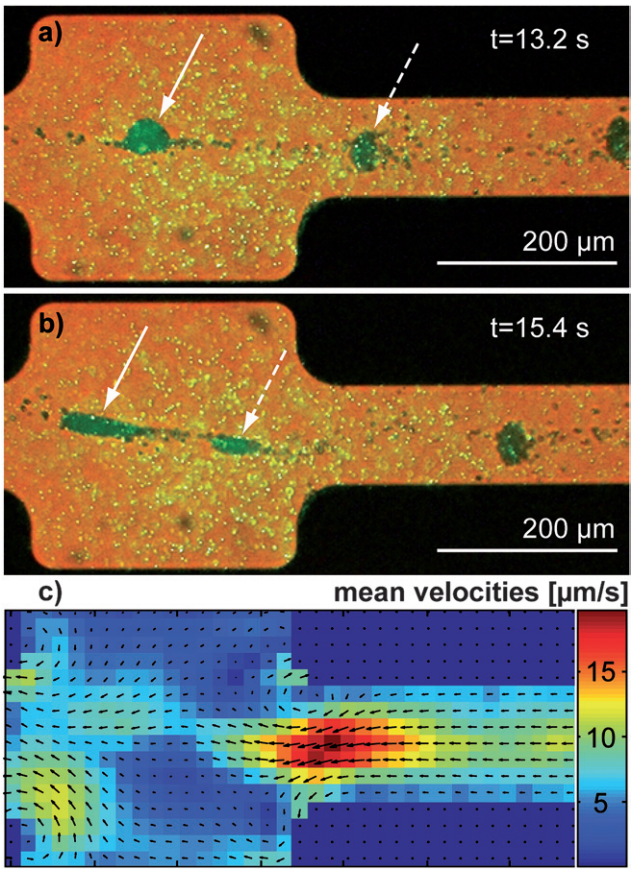

Fig. 4 (a–b): Position and shape of a caged aggregate of 5 µm green beads (marked with solid arrows) during ultrasound-mediated injection of a new aggregate (marked with dashed arrows). The images illustrate the two turning points of the oscillating displacement and shape transformation of the caged aggregate. (c): Average during 30 s (6 modulation cycles) of the fluid velocity field measured by time-resolved particle image velocimetry (PIV). All data in (a–c) are extracted from the third video sequence provided as ESI.†

HEK cell (green) caged and merged with NK cells (red) that have been ultrasonically transported into the cage (last panel). Both the green and red fluorescence are viability indicators (calcein-AM). Single cell transport is demonstrated in the second ESI video clip.†

The positioning accuracy of particles in the cage during frequency modulation is characterized in Fig. 4a–b. (The micrographs in Fig. 4a–b are selected frames from the third ESI video clip.)† Here, 5 µm beads (green) are transported (*cf.* dashed arrows) and positioned (*cf.* solid arrows) by ultrasound, while 1 µm beads (yellow) are used as fluid trackers as they are small enough for the viscous drag to dominate over the acoustic forces.[15] The caged aggregate is repeatedly transformed between spheroid-shaped (Fig. 4a) and elongated (Fig. 4b). Simultaneously, the center of gravity of the aggregate oscillates with amplitude 20–30 µm and period 5 s (*i.e.* the period of the 0.2 Hz modulation frequency), while the maximum displacement of an individual bead in the aggregate is ~80 µm. Similar position oscillations as for the center of gravity are seen for individual cells in the cage. (Single cell transport is demonstrated in the second ESI video clip.)†

The fluid motion caused by the ultrasound-mediated transport was characterized by time-resolved particle image velocimetry (PIV) on the same video sequence as seen in Fig. 4a–b, but on the full 30 s interval. The PIV calculations were performed on processed images suppressing anything but yellow pixel values (which display the 1 µm beads). Fig. 4c shows the time-averaged velocities of the fluid flow over six cycles of 0.2 Hz modulation within the same imaged area as seen in Fig. 4a–b. (Time-resolved PIV results are provided in the fourth ESI video clip.)†

Discussion and conclusion

Spatial stabilization of ultrasonic alignment forces in microfluidic chips is important in applications requiring accurate transport of particles or cells at low or moderate speeds (<1 mm s^{-1}). The principle is based on averaging the force fields obtained from different fixed actuation frequencies. For example, fixed-frequency operation may cause an aligned cell entering a "blind spot" (*cf.* Fig. 2) to settle by gravity and adhere to the channel bottom. Such settlement of HEK or NK cells typically has a sedimentation time of ~10 s in our system.[15] Furthermore, areas of "de-alignment" (*cf.* Fig. 2) may drive the cells to the channel wall within less than one second. Thus, at flow (and/or transport) velocities up to ~0.1 mm s^{-1} there is a significant risk of particle-to-wall contact during fixed-frequency ultrasonic alignment, leading to, *e.g.*, contamination, clogging or loss of sample. We have also noted that the ultrasonic resonances are sensitive to how the transducer is placed on the chip. Small changes in transducer position and orientation also change the force field pattern, which, in turn, requires manual selection of the best operating frequency from one experiment to another. Furthermore, similar experiments as presented in Fig. 2 show that the alignment performance changes with temperature. For example, the relative length of the blind spots changed from 58 to 45% when the temperature of the microscope stage was increased from 23 to 37 °C (data not shown). All these limitations associated with fixed-frequency ultrasonic actuation can be eliminated with a properly chosen frequency modulation scheme.

Ultrasound-mediated transport in microchannels is an attractive and simple approach for flow-free control of the motion and position of individual particles or cells. The principle is based on ultrasonic arraying[11] of particles (*i.e.* grouping particles along the channel in a 1D array) followed by translation of the trapping sites in the array by a slow frequency sweep within a suitably selected frequency interval. The frequency sweep interval must be chosen so that, at the end of a sweep, the position of a trapping site is closer to the "next" site of the starting frequency than it is to the one where the particle(s) were at the beginning of the sweep. Our demonstrated method shows promise for high flexibility and precision: The particle speed is controlled by the modulation frequency (*cf.* inset in Fig. 3b), and the direction of motion can be reversed by switching the sweep direction (*i.e.*, from positive to negative slope of the sawtooth-shaped frequency sweep). (Demonstration of reversed transport is provided in the first ESI video clip.)† By simultaneously performing rapid modulation (for alignment stabilization) and slow modulation (for transport), it is possible to move the particles along the full channel length of 5 mm, away from the channel boundaries and within the focal plane of the microscope. In addition, by avoiding particle transport based on fluid pumping, common problems such as unwanted transient flows after a pump is started or stopped are eliminated. On the other hand, there is also a possibility to move particles or cells and the fluid at different speeds independently of each other by the use of combined ultrasound- and pump-mediated transport. One observed limitation of the method arises when transporting high-concentration samples of particles or cells (*cf.* Fig. 3a). Under such circumstances some particles may "leak" from one aggregate to an adjacent aggregate. (This effect can be seen in the first ESI video clip.)† One possible reason for this effect is the limited size of the trapping sites in the 1D array, limiting the maximum number of particles in each aggregate that can be transported. This hypothesis is supported when studying single-cell transport, where the effect is not present. (Provided in the second ESI video clip.)†

In the future we aim for utilizing the device for monitoring intercellular interactions between NK or T cells and their target cells (such as HEK or B cells). A proof-of-concept experiment for this application is provided in Fig. 3c. For example, a controlled number of target cells may be injected into the cage one-by-one by the slow-frequency-modulation method, and merged with a pre-injected NK cell. Here, dynamic studies of the intercellular interactions may be performed, and correlated with, *e.g.*, the number of neighbors for each cell in the aggregate,[13] or with stimuli from various soluble agents provided *via* microfluidic perfusion. Additionally, the flow-free transport approach also makes it possible to inject a cell into the cage without considerably diluting or removing any molecules diffusing in the cage compartment (such as signaling molecules produced by another pre-injected cell). However, as indicated in Fig. 4 the positioning performance during slow frequency modulation is not as accurate as for fixed-frequency actuation.[13] Although there is no net displacement of caged cells, the maximum temporary displacement of individual cells is typically 50 μm (*cf.* Fig. 4a–b). Furthermore, local fluid flows exist with average velocities up to 20 μm s^{-1} (*cf.* red areas in Fig. 4c). The local flows originate partly from acoustic streaming vortices[12] and partly from fluid dragged along with a transported aggregate. (This effect can be seen in the fourth ESI video clip.)† However, around the center of the cage where cells are positioned, the average velocity of the fluid flow is less than 10 μm s^{-1}. This is one order of magnitude below the ultrasound-mediated transport speed, and of the same order as the molecular diffusion speed in a fluid at room temperature. In applications where true zero-flow or high positioning accuracy are important, the frequency modulation should be stopped when the transport and injection of cells into the cage are completed.

In this context, it should also be noted that ultrasonic manipulation in microfluidic systems has proven to be a biocompatible method allowing long-term (>1 h) monitoring of trapped cells.[16,17] In a larger perspective, we believe that ultrasound-actuated microsystems in the future could serve as simple and gentle multi-purpose tools applicable to a wide variety of cell handling tasks.

Acknowledgements

The authors thank Prof. H. M. Hertz for valuable discussions and for contributions to the original idea of this work. Financial support is gratefully acknowledged from the Swedish Research Council and the Göran Gustavsson Foundation.

References

1 J. Atencia and D. J. Beebe, *Nature*, 2005, **437**, 648–655.
2 G. Medoro, R. Guerrieri, N. Manaresi, C. Nastruzzi and R. Bambari, *IEEE Des. Test. Comput.*, 2007, **24**, 26–36.
3 P. Y. Chiou, A. T. Ohta and M. C. Wu, *Nature*, 2005, **436**, 370–372.

4 T. Laurell, F. Petersson and A. Nilsson, *Chem. Soc. Rev.*, 2007, **36**, 492–506.
5 M. Wiklund and H. M. Hertz, *Lab Chip*, 2006, **6**, 1279–1292.
6 G. Whitworth, M. A. Grundy and W. T. Coakley, *Ultrasonics*, 1991, **29**, 439–444.
7 T. Kozuka, T. Tuziuti and H. Mitome, Proceedings of 11th IEEE International Symposium on Micromechatronics and Human Science, 2000, pp. 201–206.
8 S. Oberti, A. Neild and J. Dual, *J. Acoust. Soc. Am.*, 2007, **121**, 778–785.
9 T. L. Tolt and D. L. Feke, *Chem. Eng. Sci.*, 1993, **48**, 527–540.
10 M. Saito, N. Kitamura and M. Terauchi, *J. Appl. Phys.*, 2002, **92**, 7581–7586.
11 O. Manneberg, J. Svennebring, H. M. Hertz and M. Wiklund, *J. Micromech. Microeng.*, 2008, **18**, 095025 (9 pp).
12 S. M. Hagsäter, A. Lenshof, P. Skafte-Pedersen, J. P. Kutter, T. Laurell and H. Bruus, *Lab Chip*, 2008, **8**, 1178–1184.
13 O. Manneberg, B. Vanherberghen, J. Svennebring, H. M. Hertz, B. Önfelt and M. Wiklund, *Appl. Phys. Lett.*, 2008, **93**, 063901 (3 pp).
14 http://www.oceanwave.jp/softwares/mpiv/.
15 O. Manneberg, S. M. Hagsäter, J. Svennebring, H. M. Hertz, J. P. Kutter, H. Bruus and M. Wiklund, *Ultrasonics*, 2009, **49**, 112–119.
16 J. Hultström, O. Manneberg, K. Dopf, H. M. Hertz, H. Brismar and M. Wiklund, *Ultrasound Med. Biol.*, 2007, **33**, 145–151.
17 M. Evander, L. Johansson, T. Lilliehorn, J. Piskur, M. Lindvall, S. Johansson, M. Almqvist, T. Laurell and J. Nilsson, *Anal. Chem.*, 2007, **79**, 2984–2991.